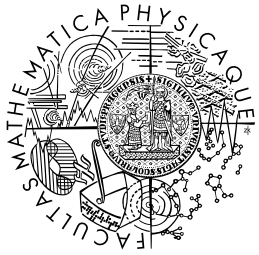

FACULTY
OF MATHEMATICS
AND PHYSICS
Charles University

BACHELOR THESIS

David Vokrouhlický

Short-lived Delocalization and Absorption by Light

Institute of Physics, Charles University

Supervisor of the bachelor thesis: doc. Mgr. Tomáš Mančal, Ph.D.
Study programme: Physics
Study branch: General physics

Prague 2020

I declare that I carried out this bachelor thesis independently, and only with the cited sources, literature and other professional sources. It has not been used to obtain another or the same degree.

I understand that my work relates to the rights and obligations under the Act No. 121/2000 Sb., the Copyright Act, as amended, in particular the fact that the Charles University has the right to conclude a license agreement on the use of this work as a school work pursuant to Section 60 subsection 1 of the Copyright Act.

In Prague date 4.6.2020 David Vokrouhlický

Author's signature

I would like to thank my supervisor doc. Tomáš Mančal for his patient guidance and thoughtful insights.

Název práce: Krátkočasová delokalizace a absorpce světla

Autor: David Vokrouhlický

Katedra: Fyzikální ústav Univerzity Karlovy

Vedoucí bakalářské práce: RNDr. Tomáš Mančal, Ph.D., Fyzikální ústav Univerzity Karlovy

Abstrakt: Koherentní delokalizace excitonů zlepšuje funkci sběru světla fotosyntetických antén tím, že vytváří podmínky pro velmi rychlý přenos excitace v prostoru. Tato práce se zaměřuje na dva různé efekty vytvářející koherenci - krátkodobé excitace světlem a slabou vazbu mezi pigmenty, které jsou v systému přítomny v delším časovém měřítku. Je vypočten vývoj a relaxace jednoduchých systémů - dimeru a trimeru. Hlavní část práce prezentuje nové numerické metody pro rozlišení dvou typů koherence v průběhu evoluce, a jejich aplikaci na zmíněné systémy.

Klíčová slova: Molekulární systémy, kvantová mechanika, spektroskopie

Title: Short-lived Delocalization and Absorption by Light

Author: David Vokrouhlický

Institute: Institute of Physics, Charles University

Supervisor: doc. Mgr. Tomáš Mančal, Ph.D., Institute of Physics, Charles University

Abstract: Coherent exciton delocalization improves the light harvesting function of photosynthetic antennae by creating conditions for very fast excitation transfer in space. This thesis focuses on two different effects creating coherence - short-lived excitation by light and weak coupling between pigments that is present in the system on longer timescales. The evolution and relaxation of simple systems - the dimer and trimer - are calculated. The core of this thesis are newly developed numerical methods for distinguishing and quantifying the effect of the two types of coherence throughout evolution, which are applied to the aforementioned systems.

Keywords: molecular systems, quantum mechanics, spectroscopy

Contents

Introduction

In the past decade, the topic of coherence and its role in fast electronic energy transfer in photosynthetic systems has been a centerpiece of the field of photosynthetic study. There have been many papers quantifying coherence and demonstrating its role in efficient energy transfer [4],[1], [11]. Coherence, however, is a consequence of both inter-site coupling and the excitation by an external field. In a strictly mathematical sense, these two coherences are equivalent and both their contributions intertwine as the system evolves in time.

This thesis aims at distinguishing these two types of coherences using newly developed numerical methods to analyze the system evolution. In Chapter 1, the theoretical model of energy transfer in photosynthetic antennae is outlined with a simple form of interaction with a thermodynamic bath environment. The evolution and relaxation of a dimer is calculated. In Chapter 2, the concept of the two types of coherences is discussed in depth and possible ways of their quantification are proposed. In Chapter 3, the application of the proposed numerical quantification methods of separating these two contributions to coherence is illustrated by analyzing simple dimer and trimer systems.

As the role of coherence in fast energy transfer is still under discussion, it is important to distinguish different sources of coherence in order to correct interpret both experimental data and data from numerical simulations. The numerical methods developed in this thesis could potentially be used precisely in that matter.

1. Theoretical model

In this chapter the structure and assumptions of the studied model will be outlined. The aggregate Hamiltonian and a simple form of system-bath interaction will be derived.

1.1 Aggregate Hamiltonian

Photosynthetic antennae consist of several chlorophyll molecules, which can be modeled with sufficient accuracy as two-level systems for small levels of site excitation. The single excitation restriction is commonly employed in the field of photosynthesis study, as higher orders of excitation are only reached with levels of excitation larger than present during excitation by natural sunlight, and are also not easily accessible by standard spectroscopic measurements.

Firstly, we construct the Hamiltonian of the system alone, taking into account energies of excited states and coupling between sites. In the localized site basis, where $|i\rangle_{i=1}^{N}$ denotes the ith site excited with all others in the ground state, the Hamiltonian has a simple form

$$H_S = \sum_{i=1}^{N} \varepsilon_i |i\rangle\langle i| + \sum_{i=1}^{N}\sum_{j>i}^{N} J_{ij}(|i\rangle\langle j| + |j\rangle\langle i|), \tag{1.1}$$

where ε_i are the site energies and J_{ij} is the inter-site coupling, which can be approximated by dipole-dipole interaction, if the distances between sites r_{ij} are large enough

$$J_{ij} = \frac{1}{4\pi\epsilon_0 r_{ij}^3}\left[\boldsymbol{\mu}_i \cdot \boldsymbol{\mu}_j - 3\frac{(\boldsymbol{\mu}_i \cdot \mathbf{r}_{ij})\,(\mathbf{r}_{ij} \cdot \boldsymbol{\mu}_j)}{r_{ij}^2}\right]. \tag{1.2}$$

Since the wavelength of incoming light is much larger than the scale of the system, the light-matter interaction can be treated semiclassically in the dipole approximation, with the interaction Hamiltonian for each site being

$$H_{el} = -\boldsymbol{\mu} \cdot \mathbf{E}, \tag{1.3}$$

where $\boldsymbol{\mu}$ is the dipole moment operator of the site, and $\mathbf{E}$ is the electric field of incoming light. In the case of laser induced excitation, the field will be monochromatic, $\boldsymbol{E} = \mathbf{e}E(t)\cos(\Omega t)$, with frequency Ω, wave envelope $E(t)$ and polarization $\mathbf{e}$.

The frequency of the incoming light Ω is of similar magnitude as the characteristic frequencies of the system $\varepsilon_i/\hbar$ - there arise rapidly oscillating terms with frequencies equal to the sum of the two frequencies. The contribution of these terms when integrated is small, so they are commonly omitted. This approximation is called the rotating wave approximation.

Since the aggregate is in a protein bath environment, it is also necessary to work with the degrees of freedom of the bath, as they affect the dynamics of the system. We are, however, only interested in the dynamics and time evolution of

the system, not of the bath. It is therefore convenient to work with the so-called reduced density matrix for the system

$$\rho(t) = \mathrm{Tr}_B\{W\}, \tag{1.4}$$

where the trace of the total density matrix W is done over the bath. The density matrix formalism is also useful for describing mixed states, as opposed to solely pure state dynamics, and will be used throughout this thesis.

1.2 The Lindblad master equation

In general, when dealing with an open quantum system, the dynamics are determined not by the Schrödinger (Liouville-von Neumann) equation, but rather by a quantum master equation, which takes into account dissipative effects. Its general form is [10]

$$\frac{\partial}{\partial t}\rho(t) = -\frac{i}{\hbar}\left[H, \rho(t)\right] - \mathcal{R}(t)\rho(t), \tag{1.5}$$

where $\mathcal{R}$ is the relaxation tensor, which is a 4th rank tensor that describes effects such as dephasing or population relaxation.

A useful and accurate approach is the Markov approximation, where the bath has a "short memory", meaning that its correlation time is short. The most general Markov master equation is the Lindblad master equation. With the Markov approximation, we can write the time depenent state using a propagator:

$$\rho(t) = \mathcal{V}(t)\rho(t_0). \tag{1.6}$$

The propagator $\mathcal{V}$ has to fulfill the semigroup property

$$\mathcal{V}(t_2)\mathcal{V}(t_1) = \mathcal{V}(t_2 + t_1). \tag{1.7}$$

The solution to this condition is an exponential form

$$\mathcal{V}(t) = \exp(\mathcal{L}t). \tag{1.8}$$

It has been shown, that the superoperator $\mathcal{L}$ has to be in the Lindblad form [5]

$$\frac{\partial}{\partial t}\rho(t) = \mathcal{L}(\rho) = -\frac{i}{\hbar}[H, \rho] + \sum_k \gamma_k \left[L_k \rho L_k^\dagger - \frac{1}{2}\left\{L_k^\dagger L_k, \rho\right\}\right], \tag{1.9}$$

where H represents unitary dynamics of the system and L_k are arbitrary operators, with $\gamma_k > 0\ \forall k$ being transfer rates of different channels described by the L_k operators. These are commonly called Lindblad jump operators. For a formal derivation of the Lindblad superoperator, see Appendix A.

It is important to note that γ_k represents the rate of relaxation, whereas L_k represents the direction of relaxation. Without Lindblad terms, the equilibrium state of the system would be

$$\rho_s^{\mathrm{eq}} = e^{-\beta \mathbf{H}_s}/Z_s, \tag{1.10}$$

where $\beta = 1/kT$, k is the boltzmann constant and $Z_s = \mathrm{Tr}\left(e^{-\beta \mathbf{H}_s}\right)$ is the partition sum. Because of the relaxation that does not necessarily have to be in the direction of the system eigenbasis, the equilibrium with a Lindbladian is generally perturbed from the equilibrium in eq. (1.10). In ref.[2], this difference is calculated using second order perturbative methods, in this thesis, the approach to quantifying this difference will be numerical.

1.3 Excitonically coupled heterodimer in a bath

As an example of the Lindblad superoperator acting on a photosynthetic system, a system with two sites will be examined. A physical heterodimer is a system of two molecules interacting electrostatically with different energies of their respective excited states ϵ_1 and ϵ_2. The coupling between these two-level systems is J. When the system Hamiltonian is diagonalized, the resulting eigenstates include the ground state and two exciton states, that are formed as linear combinations of excited site states. Let the ordered energies of these two states be E_1 and E_2. If we denote the energy difference of excited site states as $\delta = \epsilon_2 - \epsilon_1$, then the eigen-energies can be written as [12]

$$E_1 = \frac{\epsilon_2 + \epsilon_1}{2} + J\sqrt{1+\Gamma^2}, \quad E_2 = \frac{\epsilon_2 + \epsilon_1}{2} - J\sqrt{1+\Gamma^2}, \tag{1.11}$$

where $\Gamma = \delta/2J$. It is common to introduce the mixing angle α as

$$\tan 2\alpha = \frac{1}{\Gamma}. \tag{1.12}$$

The eigenstates can be written as $|\psi\rangle = \cos\alpha\,|1\rangle + \sin\alpha\,|2\rangle$, for the two solutions to eq. (1.13), where $|1\rangle$ and $|2\rangle$ are the excited site states.

Firstly, let us consider the case where the Lindblad jump operators provide relaxation between the eigenstates of the Hamiltonian. There are three possible dissipate channels - from the first exciton state to the ground state, from the second exciton state to the ground state and from the second exciton state to the first exciton state. Relaxation to the ground state commonly occurs in the timescale of nanoseconds as opposed to picosecond dephasing times of the decay from the second excited state to the first. Therefore, in this model, only the exchange between excitons will be considered, and the equilibrium at the end of the evolutions is only a quasiequilibrium living for several nanoseconds.

In order for the model to be compatible with thermodynamics, the rates of the transition up and down must obey Boltzmann statistics [3], i.e.

$$\gamma_{12} = \gamma_{21} \exp\left(-\frac{\omega_{12}\hbar}{kT}\right), \tag{1.13}$$

where γ_{21} and γ_{12} denote relaxation rates from the second exciton state to the first and vice versa, $\omega_{12} = (E_2 - E_1)/\hbar$ and T is the absolute temperature. Therefore, an upward channel is also considered.

When working in the eigenbasis of the electronic Hamiltonian, the Lindblad operators L_k from eq. (1.9) providing relaxation from state m to state n have the simple form $L_{mn} = |m\rangle\langle n|$.

The Lindblad master equation for relaxation of the heterodimer after being excited by a short laser pulse with the two mentioned relaxation channels with rates ($\gamma_{10}, \gamma_{20} = 0$ and $\gamma_{21}, \gamma_{12} > 0$) can be written in the density matrix formalism in the eigenbasis where $|0\rangle$ is the ground state and $|1\rangle$ and $|2\rangle$ are the exciton states as

$$\dot{\rho} = -\frac{i}{\hbar}[H_S, \rho] - \frac{\gamma_{21}}{2}\begin{pmatrix} 0 & 0 & \rho_{02} \\ 0 & -2\rho_{22} & \rho_{12} \\ \rho_{20} & \rho_{21} & 2\rho_{22} \end{pmatrix} - \frac{\gamma_{12}}{2}\begin{pmatrix} 0 & \rho_{01} & 0 \\ \rho_{10} & 2\rho_{11} & \rho_{12} \\ 0 & \rho_{21} & -2\rho_{11} \end{pmatrix}. \tag{1.14}$$

The ground state is not relevant in the phenomena being introduced in this thesis and can be calculated as $\rho_{00} = 1 - \rho_{11} - \rho_{22}$ if needed - it is therefore not considered in the following calculations. The explicit representation of the Lindblad superoperator in Liouville space is

$$\begin{pmatrix} \dot{\rho_{11}} \\ \dot{\rho_{22}} \\ \dot{\rho_{01}} \\ \dot{\rho_{02}} \\ \dot{\rho_{12}} \end{pmatrix} = \begin{pmatrix} -\gamma_{12} & \gamma_{21} & 0 & 0 & 0 \\ \gamma_{12} & -\gamma_{21} & 0 & 0 & 0 \\ 0 & 0 & \frac{i}{\hbar}E_1 - \frac{\gamma_{12}}{2} & 0 & \\ 0 & 0 & 0 & \frac{i}{\hbar}E_2 - \frac{\gamma_{21}}{2} & 0 \\ 0 & 0 & 0 & 0 & \frac{i}{\hbar}(E_2 - E_1) - \frac{\gamma_{12}+\gamma_{21}}{2} \end{pmatrix} \begin{pmatrix} \rho_{11} \\ \rho_{22} \\ \rho_{01} \\ \rho_{02} \\ \rho_{12} \end{pmatrix} \tag{1.15}$$

From the block diagonal structure of this superoperator it can be seen that it is possible to deal with optical coherences separately, and then solve the block of sites 1 and 2 and the coherence between them.

This set of equations directly leads to the solution

$$\begin{aligned} \rho_{11} &= \frac{1}{\gamma_{12}+\gamma_{21}}\left[\gamma_{21}(\rho_{11}(0)+\rho_{22}(0)) + (\gamma_{12}\rho_{11}(0) - \gamma_{21}\rho_{22}(0))e^{-(\gamma_{12}+\gamma_{21})t}\right] \\ \rho_{22} &= \frac{1}{\gamma_{12}+\gamma_{21}}\left[\gamma_{12}(\rho_{11}(0)+\rho_{22}(0)) + (\gamma_{21}\rho_{22}(0) - \gamma_{12}\rho_{11}(0))e^{-(\gamma_{12}+\gamma_{21})t}\right] \\ \rho_{01} &= \rho_{01}(0)e^{i\frac{E_1}{\hbar}t}e^{-\frac{\gamma_{12}}{2}t} \\ \rho_{02} &= \rho_{02}(0)e^{i\frac{E_2}{\hbar}t}e^{-\frac{\gamma_{21}}{2}t} \\ \rho_{12} &= \rho_{12}(0)e^{i\frac{E_2-E_1}{\hbar}t}e^{-\frac{\gamma_{12}+\gamma_{21}}{2}t} \end{aligned} \tag{1.16}$$

This result is in accordance with ref. [8] which calculates the behavior of optical coherences. In the eigenbasis of the electronic Hamiltonian:

- **Population** of the second exciton state decays exponentially to a constant while the first exciton state is getting fed and behaves as $1 - e^{-x}$,
- **Optical coherences** exponentially decay and oscillate at the frequency of the respective energy levels,
- **Electronic coherences** exponentially decay with rates equal to the sum of the two rates and oscillate at the frequency equal to the difference of the respective energy levels.

If, however, the Lindblad operators do not represent transitions between eigenstates, but between general states rotated from the eigenbasis, the superoperator suddenly does not have the block structure. The motivation behind this rotated relaxation is to distinguish different effects that contribute to coherences and will be thoroughly discussed in Chapter 2. When the basis in which these operators are in the form $L_{mn} = |m\rangle\langle n|$ is rotated from the eigenbasis, the dynamics of

the system change. The rotation is done only on the exciton states in order to preserve the ground state:

$$R = \begin{pmatrix} 1 & 0 & 0 \\ 0 & \cos\theta & -\sin\theta \\ 0 & \sin\theta & \cos\theta \end{pmatrix}, \; L_{mn} = R|m\rangle\langle n|R^T. \tag{1.17}$$

The superoperator now contains many more off-diagonal terms and becomes very complex - non-secular dynamics arise. If we look only at the optical coherences, the master equation becomes

$$\begin{pmatrix} \dot{\rho_{01}} \\ \dot{\rho_{02}} \end{pmatrix} = \begin{pmatrix} i\frac{E_1}{\hbar} - \frac{\gamma_{12}\cos^2\theta + \gamma_{21}\sin^2\theta}{2} & -\frac{\gamma_{12}+\gamma_{21}}{4}\sin 2\theta \\ -\frac{\gamma_{12}+\gamma_{21}}{4}\sin 2\theta & i\frac{E_2}{\hbar} - \frac{\gamma_{12}\sin^2\theta + \gamma_{21}\cos^2\theta}{2} \end{pmatrix} \begin{pmatrix} \rho_{01} \\ \rho_{02} \end{pmatrix}. \tag{1.18}$$

For the exciton block, the superoperator is even more complicated - the general analytic solution is too complex to be used practically. At this point, it is more useful to plug in a specific angle θ and solve by numerical diagonalization.

2. Two types of coherences

As the role of coherence in photosynthesis is still widely discussed, it is important to understand the effects which take part in creating it. Coherence is a consequence both of inter-site coupling and the excitation by an external field. In a strictly mathematical way, these two coherences are equivalent and both their contributions intertwine as the system evolves in time.

The excitation coherence is a coherence between excitonic states. Its life time is short, not much longer than optical coherence [7]. It is not a characteristic of the system, but simply a consequence of short excitation.

On the other hand, off-diagonal elements in the density matrix are present simply as a consequence of coupling between chlorophyll molecules. Eigenstates of the Hamiltonian become delocalized and another, long-lived coherence arises. This is the coherence that is still present after the system reaches steady state - it is a characteristic of the system itself, determined by the strength of inter-site coupling.

Throughout the systems time evolution, the system has a "preferred basis" - its eigenbasis, which describes the state to which the system would relax without Lindblad terms. The Lindblad superoperator also has a "preferred basis" - meaning that the direction of the jump operators is between states of the basis ($L_{ij} = |i\rangle\langle j|$).

If the Lindblad relaxation tensor is in the eigenbasis of the system, the preferred basis is the eigenbasis for the whole time throughout the systems evolution. If, however, the Lindblad relaxation tensor has a different preferred basis than the system eigenbasis, the preferred basis of the system is "somewhere between" these two bases. It also varies in time, as does the strength of the two effects of strong excitation and relaxation. The preferred basis is essentially something like a time varying eigenbasis of the whole system with bath interaction.

Because of the combined evolution and the nature of these coherences, it is impossible to transform one of these coherences away. However, it is, in some cases, at least numerically possible to find the preferred basis of the system.

2.1 Choosing the right basis

What is the preferred basis then? It is the one where oscillation is exclusively a matter of coherences, while the diagonal density matrix elements exhibit exponential decay. To quantify this analytically, a few methods were tried out in this work.

At first, a measure using the Fourier transform was proposed. The oscillation of a function f was defined as the maximum of the Fourier transform of the function

$$o(f) = \max \mathcal{F}(f - \bar{f}) \tag{2.1}$$

where $\bar{f}$ denotes the mean value of the function in order to eliminate the peak of the Fourier transform at $\omega = 0$. The measure of how close a basis was to the preferred basis was then the sum of oscillations of site amplitudes

$$M = \sum_i o(\rho_{ii}) \tag{2.2}$$

For some cases and in some bases, notably when the relaxation was fast, in some bases the function flattened to almost a constant, and therefore had zero oscillation. It is also worthy to note the uncertainty principle for the discrete Fourier transform, which is another source of error for this method - it is important to include at least one period of all oscillatory behavior in the system.

Another way of determining how good is a basis is by looking at the second derivative of the site amplitudes. Then the oscillation of a function is defined as the sum of the lengths of all the intervals where its second derivative has a the sign that is most common for the function. For example: for a more concave function, the oscillation is defined as

$$o(f) = ||\{x, \frac{d^2 f}{dx^2} \leq 0\}||. \tag{2.3}$$

In this case the second derivative is calculated by spline interpolation followed by differentiation. This method was chosen because it is much faster than computing a numerical second derivative, while having the same results.

To assess how close is a basis to the preferred basis, the oscillations of diagonal elements are again added

$$M = \sum o(\rho_{ii}). \tag{2.4}$$

The basis that has maximal parameter M out of the test space is the preferred basis numerically found.

During the time evolution, the two previously described effects vary in strength. Right after the fast excitation, the system Hamiltonian dominates. On the longer timescale, the relaxation takes over. This effect creates a problem with determining the preferred basis - it varies in time, and so does the parameter M. To find this time dependence, it would be necessary to work only with parts of the complete time development, find the suitable basis in the specific time window, and do so for all time windows. Ideally, the window should be small, so the preferred basis time dependence is well described.

In some simple cases, the preferred basis can be determined analytically. In Chapter 1, the time evolution of a excitonically coupled dimer with relaxation between states rotated from the eigenstates was calculated. The full superoperator has been calculated, and it can be diagonalized. This result can be compared with the numerical methods of finding preferred bases to determine their precision.

When observing the preferred basis evolution, profound questions arise. Does the system "know" to which states will it relax to? Is it a characteristic of the system, or do we have to propagate the density matrix to find out? Would it be somehow possible to determine where the system will relax to from just part of the evolution?

3. Numerical simulation

In this chapter, results of the implementation of the methods discussed in Chapter 2 are demonstrated. To find the preferred basis evolution, it is firstly needed to calculate the systems time evolution throughout and after the excitation. The time evolution of the system was calculated using the *Quantarhei 0.0.57* package[6].

3.1 Excitation by a δ-pulse

In order to study only the relaxation process, it was required to simulate an excitation by a short laser pulse. The density matrix after the pulse was then used as an initial condition for all relaxation simulations. At first, short pulses were simulated, however, to get not only the correct site amplitudes, but also coherences, a clean way of excitation was implemented - the excitation by a δ-pulse.

When a delta pulse in the form of $\vec{E}(t) = \vec{E}_0 \delta\left(t - t_p\right) \frac{1}{2}\left(e^{-i\omega(t-t_p)} + e^{i\omega(t-t_p)}\right)$ is applied to a two level system, the operator which accordingly excites the system is

$$\hat{Ex} = \begin{pmatrix} \cos\frac{J_0}{\hbar} & -i\sin\frac{J_0}{\hbar} \\ -i\sin\frac{J_0}{\hbar} & \cos\frac{J_0}{\hbar} \end{pmatrix}, \tag{3.1}$$

where $J_0 = \frac{\vec{\mu}\cdot\vec{E}_0}{2}$. Since both molecules are being excited, the complete excitation operator is obtained by applying the two individual excitation operators.

$$\hat{Ex} = \hat{Ex}_1\hat{Ex}_2 = \begin{pmatrix} \cos\frac{J_1}{\hbar} & -i\sin\frac{J_1}{\hbar} & 0 \\ -i\sin\frac{J_1}{\hbar} & \cos\frac{J_1}{\hbar} & 0 \\ 0 & 0 & 1 \end{pmatrix} \cdot \begin{pmatrix} \cos\frac{J_2}{\hbar} & 0 & -i\sin\frac{J_2}{\hbar} \\ 0 & 1 & 0 \\ -i\sin\frac{J_2}{\hbar} & 0 & \cos\frac{J_2}{\hbar} \end{pmatrix} \tag{3.2}$$

For a complete derivation of the excitation operator, see Appendix B.

3.2 Dimer

A simple model system discussed in chapter 1 is the excitonically coupled dimer. Excitation by a δ-pulse and relaxation were simulated. The parameters of the simulated dimer are listed in Table 3.1.

Table 3.1: Parameters of the dimer simulation

Parameter	Value
$\epsilon_1/\hbar$	1.0 [1/fs]
$\epsilon_2/\hbar$	1.1 [1/fs]
J	0.05 [1/fs]
γ_{21}	1/20.0 [1/fs]
E_0	20 [1/fs/a.u.]
T	300K

For this system, the mixing angle is $\theta \approx 22.5°$; in the following figures, it will be highlighted with a red line if relevant to the figure. In figure 3.1 the

evolution of the dimer with relaxation according to equation (1.14) is shown in both the eigenbasis (left) and the site basis (right) - the site amplitudes and the real and imaginary parts of optical and electronic coherences are plotted. The eigenbasis evolution follows eq. (1.16). In the site basis, the site amplitudes oscillate while decaying exponentially/exponentially approach quasisteady state, in the eigenbasis, there are no oscillations, only exponential decay.

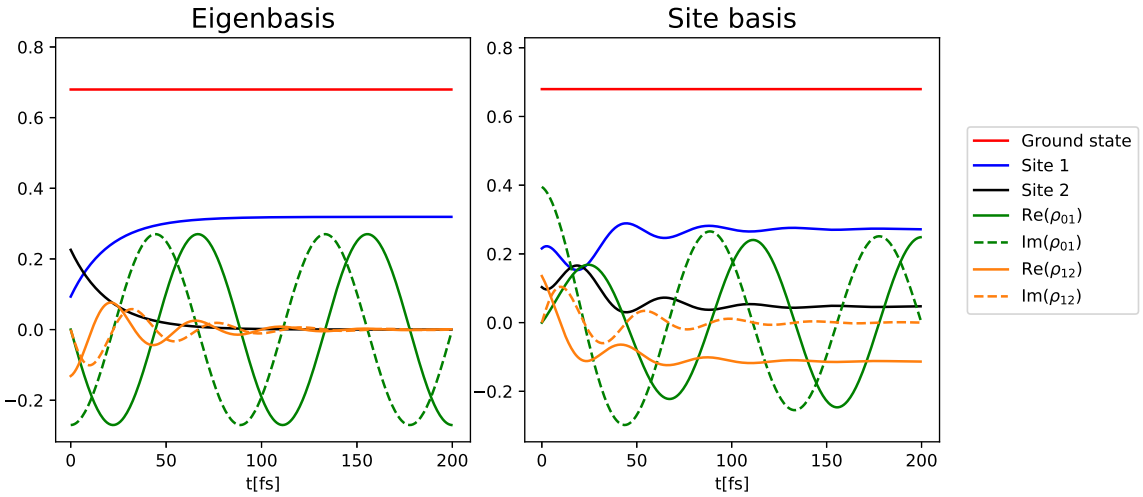

Figure 3.1: Dimer time evolution in the eigenbasis (left) and site basis (right) with relaxation between eigenstates.

When the measure described in Chapter 2 is applied to the whole evolution and bases rotated from the site basis in the range $\theta \in \langle 0, 180° \rangle$ are searched through, the eigenbasis is found - see figure 3.2. In this case, the eigenbasis is the preferred basis the whole time of the evolution.

Further on, the excitation and relaxation of a dimer with the relaxation operators rotated by $\theta = 20°$ was simulated. This evolution is shown in figure 3.3 in the site basis (right) and the numerically found preferred basis (left).

When the measure is applied to the full evolution, it is found that the basis in which the site amplitudes "oscillate the least" is rotated from the eigenbasis - even in the system eigenbasis, there are mild oscillations present. This difference is shown in figure 3.4 - the preferred basis is between the eigenbasis denoted by the red line and the basis of relaxation denoted by the green line.

The effect of the strength of relaxation on the evolution and the preferred basis was studied. In figure 3.5, the dependence of preferred basis on relaxation rate γ_{21} for coupling constants $J = 0.025, 0.05, 0.1, 0.5$ is plotted. For low levels of coupling (≤ 0.15), the relaxation is strong enough to turn the preferred basis from the eigenbasis correspondint to the particular value J. For greater coupling, the relaxation does not have such an effect in this range, for larger values of γ_{21} the method becomes inconclusive due to the fact, that relaxation is too fast.

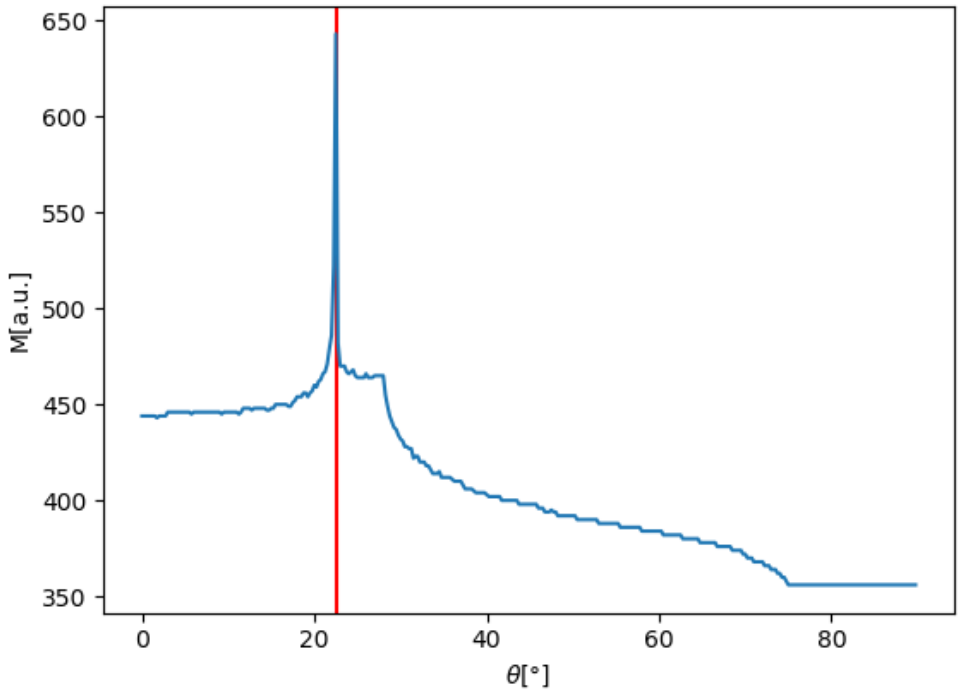

Figure 3.2: Measure of bases rotated from the site basis by angle θ in arbitrary units for non-rotated relaxation, red vertical line denotes the mixing angle, i.e. position of the eigenbasis.

3.2.1 Final state of relaxation

As was discussed in Chapter 2, it is interesting to note where does the system relax to. The basis where the quasiequilibrium endstate is diagonal should be somewhere between the eigenbasis and the basis of the relaxation operators. Relaxation was calculated for different values of γ_{21}. This relationship is plotted in figure 3.6. For different levels of γ_{21}, different total evolution times were used, so that the system manages to relax fully. There is a clear tendency to move from the eigenbasis towards the basis of the relaxation operators as γ_{21} increases. In figure 3.10, the comparison between the endstate basis and the preferred basis for different levels of relaxation described by relaxation time constants $\tau_{21} = 1/\gamma_{21}$ is plotted for different levels of coupling. It is interesting that the preferred basis gained from the measure over the whole evolution is slightly different than the diagonal basis of the end state. From this observation it is evident, that the preferred basis changes in time, as was predicted. The endstate is also closer to the basis of the relaxation operators - this underlines the idea that the preferred basis starts at the eigenbasis, when the system Hamiltonian has a greater influence, at gradually moves towards the relaxation basis.

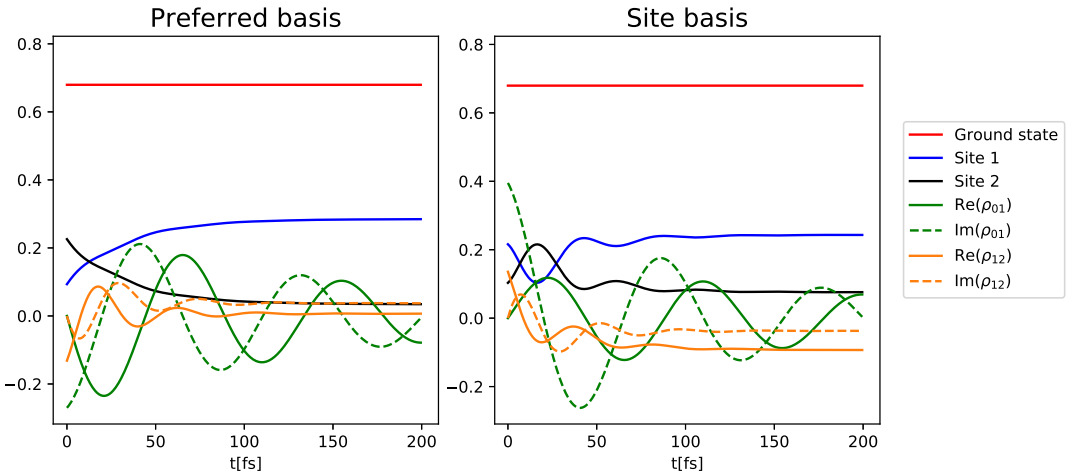

Figure 3.3: Dimer time evolution with relaxation operators rotated by 20° in the site basis (right) and in the numerically found preferred basis (left).

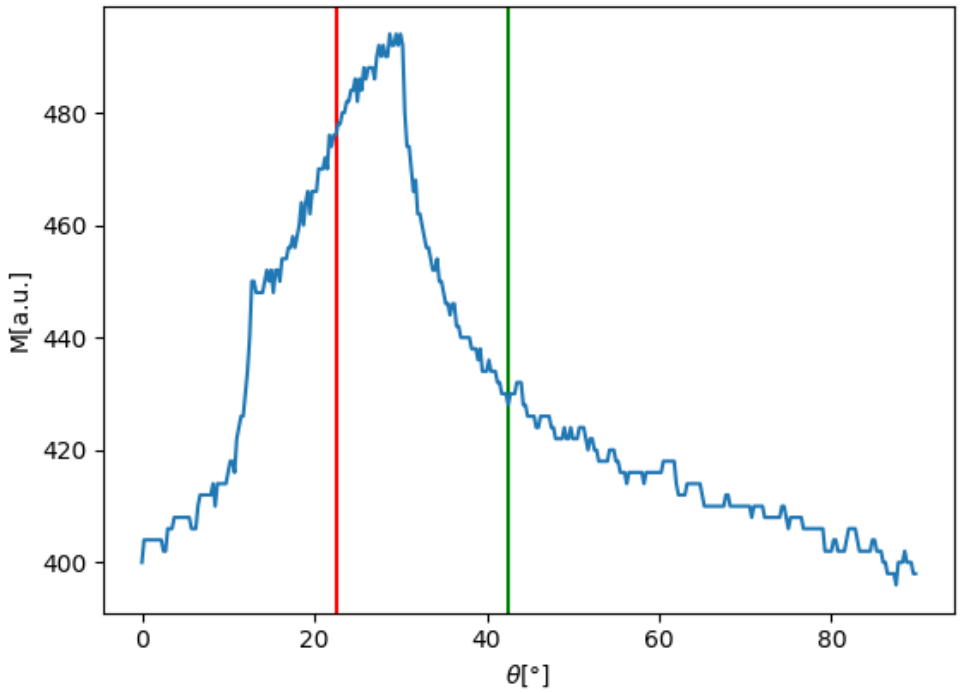

Figure 3.4: Measure of bases rotated from the site basis by angle θ in arbitrary units for relaxation rotated by 20°, red vertical line denotes the mixing angle, i.e. position of the eigenbasis, the green line is the position of the basis of relaxation.

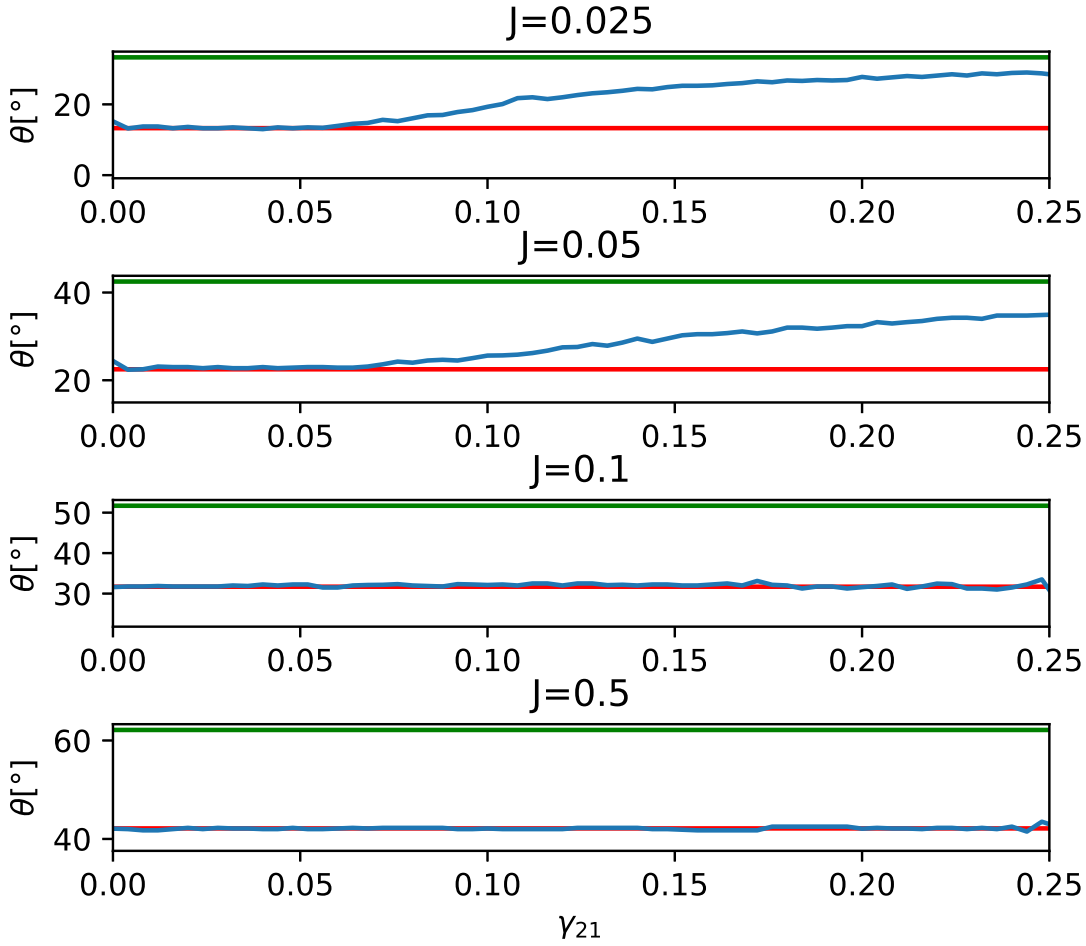

Figure 3.5: Dependence of preferred basis (blue line) on relaxation rate γ_{21} for coupling constants $J = 0.025, 0.05, 0.1, 0.5$. Red line denotes the position of the respective system eigenstates, green line denotes the basis of relaxation.

3.2.2 Window dependence

Since there is evidence of the character of the movement of the preferred basis, the method was used in different time windows throughout the evolution, as mentioned in chapter 2. The problem with the proposed method is that by choosing a window, a certain amount of periods of oscillation fit inside. The second derivative measure is then dependent more on how these waves fit in the window (i.e. their phase at the beginning and the end of the window) than on the evolution of the preferred basis. It is therefore unfortunately not possible to use this method, or the Fourier transform method, to study and see the time evolution of the preferred basis directly, or to predict the quasiequilibrium final state.

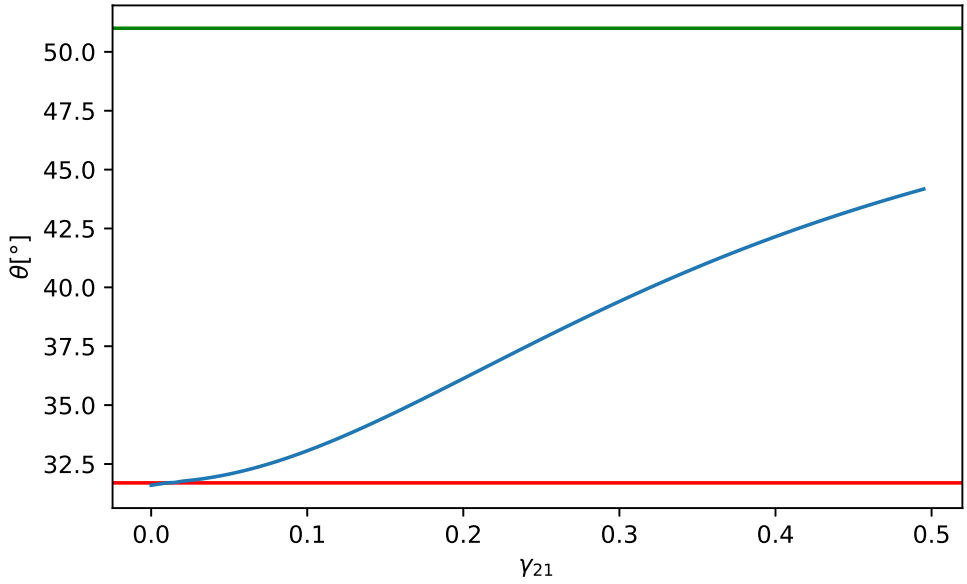

Figure 3.6: Dependency of the angle by which the diagonalized final state of relaxation is rotated from the site basis on relaxation rate. Green line denotes the basis of relaxation rotated from the eigenbasis by 20°.

3.3 Systems with more sites

Our approach can be clearly generalized to systems with more sites. The method was tested on a molecular trimer, parameters of the simulation are listed in table 3.2. Excitation was again simulated using a delta pulse. Relaxation channels

Table 3.2: Parameters of the trimer simulation

Parameter	Value
ϵ_1	1.0 [1/fs]
ϵ_2	1.05 [1/fs]
ϵ_3	1.1 [1/fs]
J_{12}	0.05 [1/fs]
J_{13}	0.05 [1/fs]
J_{23}	0.05 [1/fs]
γ_{21}	1/20.0 [1/fs]
γ_{31}	1/10.0 [1/fs]
E_0	20 [1/fs/a.u.]
T	300K

from the third and the second exciton state to the first were considered with their thermodynamically appropriate counterparts. In figure 3.8, the calculated relaxation is shown for a trimer with both relaxation operators rotated by 20° in the site basis and in the numerically found preferred basis. In figure 3.9, the use of the method is visualized for nonrotated relaxation. A slice at a certain θ_3 that corresponds to the eigenbasis is shown, a clear maximum in the other two Euler angles is found. In figure 3.10, the method results are shown on relaxation with

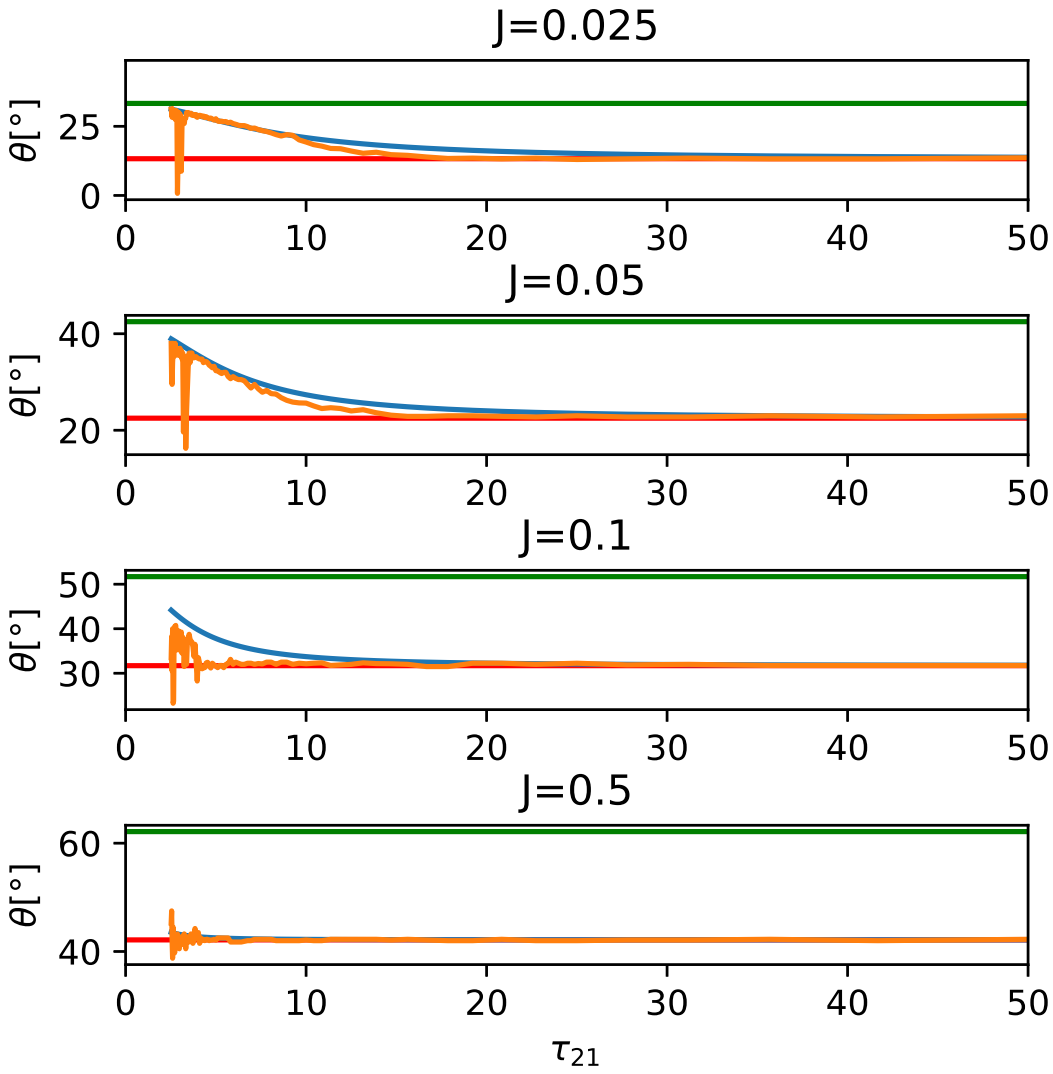

Figure 3.7: Comparison of final state of relaxation (blue line) with found preferred basis (orange) depending on relaxation time constant τ_{21} for coupling constants $J = 0.025, 0.05, 0.1, 0.5$.

both channels rotated by 20° from the eigenbasis. A slight shift of the peak in both θ_1 and θ_2 is observed, the maximum is also much less clear than in the case of simple non-rotated relaxation (as was the case with the dimer).

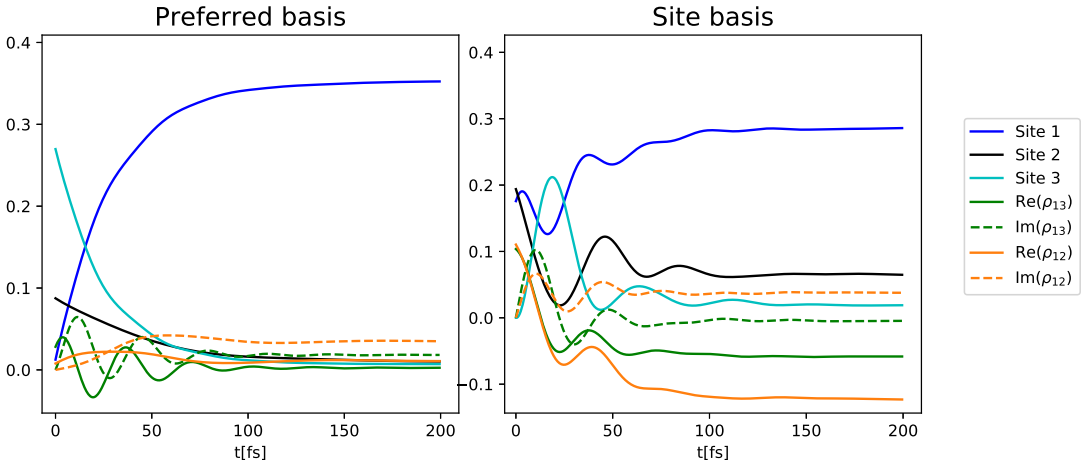

Figure 3.8: Trimer relaxation in the site basis (right) and the numerically found preferred basis (left) for relaxation rotated by 20°.

With systems consisting of more sites, the problem of finding minima efficiently arises, as the space of possible preferred bases increases in dimension. Basis rotation (as well as the eigenbasis) in n-dimensional space is generally defined by $n \cdot (n-1)/2$ parameters/angles. In the case of the trimer, these are the three Euler angles. The value that the method outputs for different angles however is not always smooth enough to implement faster optimalization algorithms, which could make finding the preferred basis much more efficient.

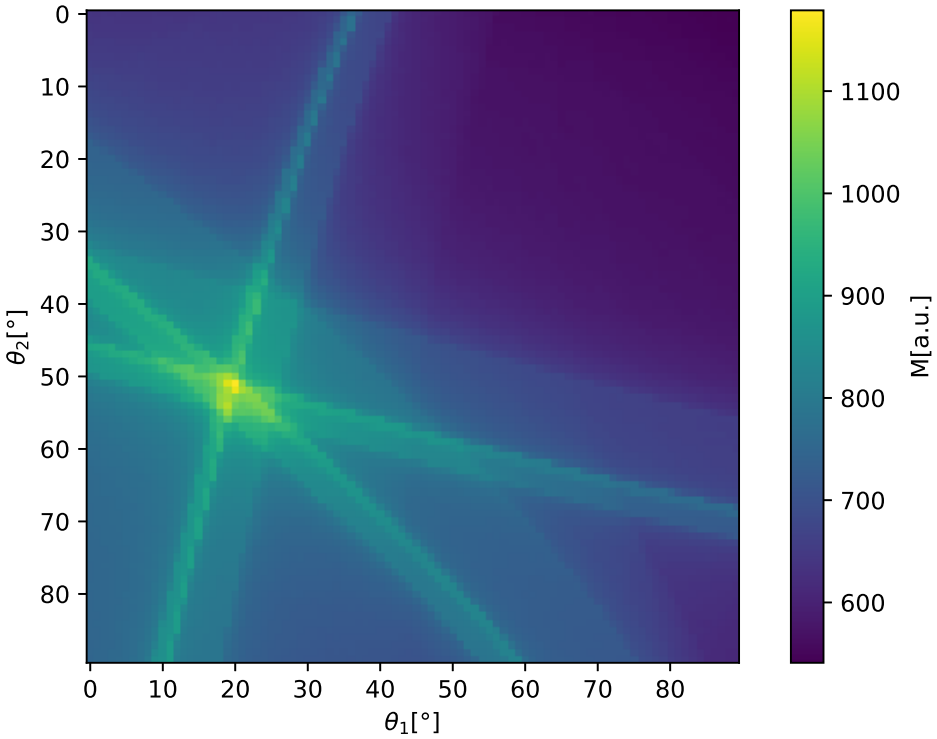

Figure 3.9: Visualization of the method for the trimer - a slice at a certain θ_3 shows the values of M for different θ_1 and θ_2, the peak corresponds to the eigenbasis of the system.

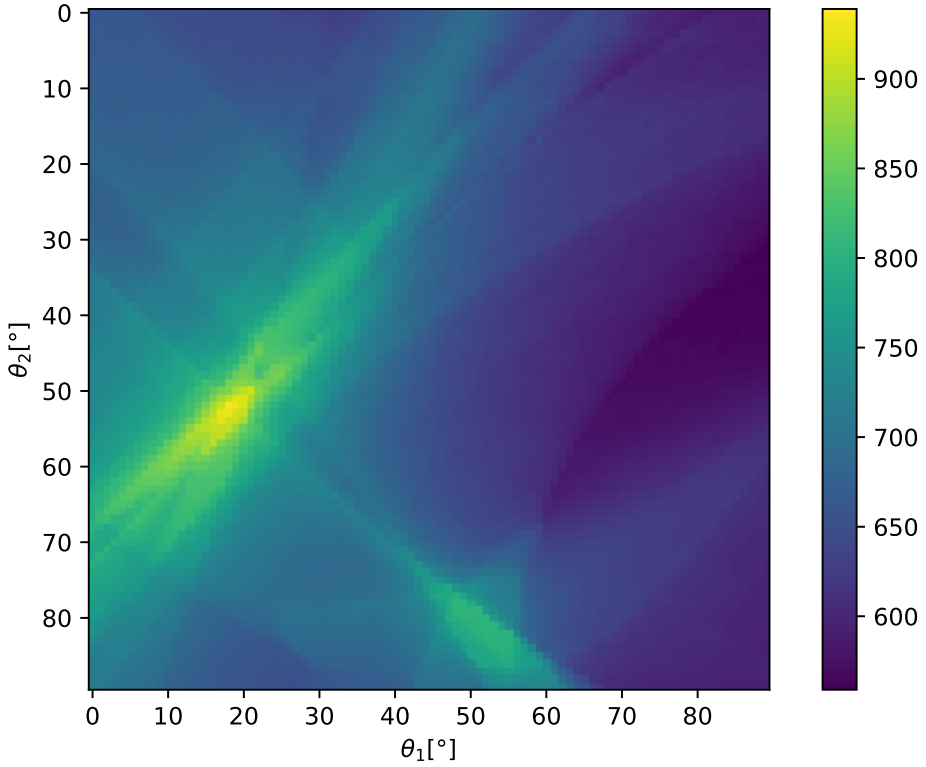

Figure 3.10: Visualization of the method for the trimer with rotated relaxation by 20° in both angles - a slice at a certain θ_3 the values of M for different θ_1 and θ_2, the peak corresponds to the numerically found preferred basis.

Conclusion

Coherence seems to play a key role in fast energy transfer in photosynthetic antennae, yet the causes for its existence are often mixed together in interpretation. In this thesis, two ways that coherence is created in chlorophyll aggregates are discussed - short-lived coherence due to excitation by light in the semiclassical approximation and exciton delocalization as a consequence of site coupling, which has a much longer lifetime. By studying the evolution of sample systems with relaxation to states rotated from the eigenstates it was possible to at least partially distinguish these two types of coherence. The concept of a preferred basis was proposed as a floating eigenbasis between the system eigenbasis and the basis of relaxation. Numerical methods for determining such a basis were developed. On the dimer system, the time evolution of such a basis was indirectly confirmed by comparing analysis of the whole evolution with the analysis of the state of the system after evolution is completed.

The numerical methods developed in this thesis could potentially be used in correctly interpreting coherence from experimental data. At this stage, the method has been successfully tested at analyzing simulated evolution of sample systems. However, in order to be more relevant to experiment, it would be needed to extend the method to analyze not just simulated evolution, but also the spectroscopic measurements directly.

Bibliography

[1] Gregory S Engel, Tessa R Calhoun, Elizabeth L Read, Tae-Kyu Ahn, Tomáš Mančal, Yuan-Chung Cheng, Robert E Blankenship, and Graham R Fleming. Evidence for wavelike energy transfer through quantum coherence in photosynthetic systems. *Nature*, 446(7137):782–786, 2007.

[2] Eitan Geva, Efrat Rosenman, and David Tannor. On the second-order corrections to the quantum canonical equilibrium density matrix. *The Journal of Chemical Physics*, 113(4):1380–1390, 2000.

[3] Josiah W. Gibbs. *Elementary principles in statistical mechanics: developed with especial reference to the rational foundation of thermodynamics*. C. Scribner's sons, 1902.

[4] Ivan Kassal, Joel Yuen-Zhou, and Saleh Rahimi-Keshari. Does coherence enhance transport in photosynthesis? *The journal of physical chemistry letters*, 4(3):362–367, 2013.

[5] Goran Lindblad. On the generators of quantum dynamical semigroups. *Communications in Mathematical Physics*, 48(2):119–130, 1976.

[6] Tomáš Mančal. *Quantarhei: Molecular Open Quantum Systems Package*. 2018.

[7] Tomáš Mančal. A decade with quantum coherence: How our past became classical and the future turned quantum. *Chemical Physics*, 532, apr 2020.

[8] Tomáš Mančal, Leonas Valkunas, Elizabeth L Read, Gregory S Engel, Tessa R Calhoun, and Graham R Fleming. Electronic coherence transfer in photosynthetic complexes and its signatures in optical spectroscopy. *Spectroscopy*, 22(2-3):199–211, 2008.

[9] Daniel Manzano. A short introduction to the lindblad master equation. *AIP Advances*, 10(2):025106, 2020.

[10] Volkhard May and Oliver Kühn. *Charge and energy transfer dynamics in molecular systems*, volume 2. Wiley Online Library, 2011.

[11] Mohan Sarovar, Akihito Ishizaki, Graham R Fleming, and K Birgitta Whaley. Quantum entanglement in photosynthetic light-harvesting complexes. *Nature Physics*, 6(6):462–467, 2010.

[12] Herbert Van Amerongen, Rienk Van Grondelle, et al. *Photosynthetic excitons*. World Scientific, 2000.

[13] Mark M Wilde. *Quantum information theory*. Cambridge University Press, 2013.

A. Derivation of the Lindbladian as a general CPT-map generator

The Lindblad superoperator can be derived from studying general Markovian transformations between density matrices. In this chapter based on Refs. [13, 9], a general form of Markovian CPT-maps and the Lindblad form will be derived.

Let $B(\mathcal{H})$ denote the space of bounded operators on a Hilbert space $\mathcal{H}$. Positivity of an operator A on a Hilbert space $\mathcal{H}$ is defined as $\langle\phi|A|\phi\rangle \geq 0, \forall|\phi\rangle \in \mathcal{H}$. Let $\rho(\mathcal{H})$ denote the space of density matrices in Hilbert space $\mathcal{H}$ (including mixed states), and $\mathcal{V} : \rho(\mathcal{H}) \to \rho(\mathcal{H})$ a map from this space onto itself. Such a map has to preserve the characteristics of density matrices: the unit trace

$$\mathrm{Tr}[\mathcal{V}\rho] = \mathrm{Tr}[\rho], \forall\rho \in \rho(\mathcal{H}) \tag{A.1}$$

and positive definity, which is a more complex condition.

Definition 1. *A map $\mathcal{V}$ is positive iff $\forall A \in B(\mathcal{H})$ s.t. $A \geq 0 \Rightarrow \mathcal{V}A \geq 0$*

This condition is, however, not sufficient. In composite states, the density matrix can be a partial trace of a larger full system density matrix. A stronger condition is needed:

Definition 2. *A map $\mathcal{V}$ is completely positive iff $\forall n \in \mathbb{N}, \mathcal{V} \otimes \mathbb{1}_n$ is positive.*

A map that is completely positive and trace-preserving is called a CPT-map for brevity. In order to derive a general form of CPT-maps on $\rho(\mathcal{H})$, we need a few theorems.

Lemma 1. *Any map $\mathcal{V} : B(\mathcal{H}) \to B(\mathcal{H})$ that can be written in the form $\mathcal{V}\rho = V^\dagger\rho V$ with $V \in B(\mathcal{H})$ is positive.*

Proof. If ρ is positive, then it can be written as $\rho = A^\dagger A$, with $A \in B(\mathcal{H})$. Therefore

$$\mathcal{V}\rho = V^\dagger\rho V \Rightarrow \left\langle\psi\middle|V^\dagger\rho V\middle|\psi\right\rangle = \left\langle\psi\middle|V^\dagger A^\dagger A V\middle|\psi\right\rangle = \|AV|\psi\rangle\| \geq 0. \tag{A.2}$$

□

Theorem 2 (Choi)**.** *A linear map $\mathcal{V} : B(\mathcal{H}) \to B(\mathcal{H})$ is completely positive iff it can be expressed as*

$$\mathcal{V}\rho = \sum_i V_i^\dagger\rho V_i \tag{A.3}$$

with $V_i \in B(\mathcal{H})$.

Proof. If $\mathcal{V}$ can be written in the form of eq. (A.3), then it is completely positive as a trivial consequence of Lemma 1.

Let d be the dimension of $\mathcal{H}$ with basis $|i\rangle$. Now we define another Hilbert space $\mathcal{H}_A$ of the same dimension with basis $|i\rangle_A$. A maximally entangled state in $\mathcal{H}_A \otimes \mathcal{H}$ is defined as

$$|\Gamma\rangle \equiv \sum_{i=0}^{d-1} |i\rangle_A \otimes |i\rangle. \tag{A.4}$$

The map $\mathcal{V}$ can be extended onto the bipartition of the two Hilbert spaces as $\mathcal{V}' : \mathcal{H}_A \otimes \mathcal{H} \to \mathcal{H}_A \otimes \mathcal{H}$:

$$\mathcal{V}' \equiv \mathbb{1}_{\mathcal{B}(\mathcal{H}_\mathcal{A})} \otimes \mathcal{V}. \tag{A.5}$$

Since $\mathcal{V}$ is completely positive, $\mathcal{V}'$ is positive. Applying $\mathcal{V}'$ to the previously defined maximally entangled state results in

$$\mathcal{V}'|\Gamma\rangle\langle\Gamma| = \sum_{i,j=0}^{d-1} |i\rangle\langle j| \otimes \mathcal{V}|i\rangle\langle j|. \tag{A.6}$$

To see the action of the map on a vector $|\psi\rangle \in \mathcal{H}_A \otimes \mathcal{H}$ we expand it into a basis

$$|\psi\rangle = \sum_{i,j=0}^{d-1} \alpha_{ij} |i\rangle_A \otimes |j\rangle. \tag{A.7}$$

Finally, we can define $V_{|\psi\rangle} \in \mathcal{B}(\mathcal{H})$ as a transformation from $|\Gamma\rangle$ to $|\psi\rangle$. Explicitly

$$\begin{aligned}
\left(\mathbb{1}_A \otimes V_{|\psi\rangle}\right)|\Gamma\rangle &= \sum_{i,j=0}^{d-1} \alpha_{ij} \left(\mathbb{1}_A \otimes |j\rangle\langle i|\right) \left(\sum_{k=0}^{d-1} |k\rangle \otimes |k\rangle\right) \\
&= \sum_{i,j,k=0}^{d-1} \alpha_{ij}(|k\rangle \otimes |j\rangle)\langle i|k\rangle = \sum_{i,j,k=0}^{d-1} \alpha_{ij}(|k\rangle \otimes |j\rangle)\delta_{i,k} \\
&= \sum_{i,j=0}^{d-1} \alpha_{ij}|i\rangle \otimes |j\rangle = |\psi\rangle.
\end{aligned} \tag{A.8}$$

This way it is possible to relate vectors from $\mathcal{H}_A \otimes \mathcal{H}$ to operators acting on $\mathcal{H}$. Going back to the extended map $\mathcal{V}'$, since it is positive, its action on $|\Gamma\rangle\langle\Gamma|$ can be decomposed as

$$\mathcal{V}'(|\Gamma\rangle\langle\Gamma|) = \sum_{l=0}^{d^2-1} |v_l\rangle \langle v_l|, \tag{A.9}$$

with $|v_l\rangle \in \mathcal{H}_A \otimes \mathcal{H}$. As before, these are related to operators on $\mathcal{H}$ as

$$|v_l\rangle = (\mathbb{1}_A \otimes V_l)|\Gamma\rangle. \tag{A.10}$$

Now it is possible to calculate the product of arbitrary $|i\rangle_A \in \mathcal{H}_A$ with $|v_l\rangle$

$$\langle i|_A |v_l\rangle = \langle i|_A (\mathbb{1}_A \otimes V_l)|\Gamma\rangle = V_l \sum_{k=0}^{d-1} \langle i|k\rangle_A \otimes |k\rangle. \tag{A.11}$$

To get the general form of a CP-map, we apply $\mathcal{V}$ to a basis element $|i\rangle\langle j|$ of $\mathcal{B}(\mathcal{H})$. Using previous results we get

$$\begin{aligned}\mathcal{V}(|i\rangle\langle j|) &= (\langle i|_A \otimes \mathbb{1}_A)\, \mathcal{V}_2(|\Gamma\rangle\langle\Gamma|)\, (|j\rangle_A \otimes \mathbb{1}_A) \\ &= (\langle i|_A \otimes \mathbb{1}_A) \left[\sum_{l=0}^{d^2-1} |v_l\rangle\langle v_l|\right] (|j\rangle_A \otimes \mathbb{1}_A) \\ &= \sum_{l=0}^{d^2-1} \left[(\langle i|_A \otimes \mathbb{1}_A)\, |v_l\rangle\right] \left[\langle v_l|\, (|j\rangle_A \otimes \mathbb{1}_A)\right] = \sum_{l=0}^{d^2-1} V_l|i\rangle\langle j|V_l.\end{aligned} \tag{A.12}$$

Expanding ρ into this basis we get the desired result

$$\mathcal{V}\rho = \sum_{l=0}^{d^2-1} V_l^\dagger \rho V_l. \tag{A.13}$$

□

Choi's theorem decribes the most general form of CP-maps. For CPT-maps, we need another constraint.

Theorem 3 (Choi-Kraus)**.** *A linear map $\mathcal{V} : B(\mathcal{H}) \to B(\mathcal{H})$ is completely positive and trace-preserving iff it can be expressed as*

$$\mathcal{V}\rho = \sum_i V_i^\dagger \rho V_i \tag{A.14}$$

with $V_i \in B(\mathcal{H})$ and

$$\sum_l V_l V_l^\dagger = \mathbb{1}_{\mathcal{H}}. \tag{A.15}$$

Proof. Choi's theorem ensures complete positiveness. It is only needed to prove that only under condition (A.15) the map is also trace-preserving. If $\mathcal{V}$ can be expressed as in (A.4), then it preserves trace using cyclic properties of the trace

$$\mathrm{Tr}[\mathcal{V}\rho] = \mathrm{Tr}\left[\sum_{l=0}^{d^2-1} V_l \rho V_l^\dagger\right] = \mathrm{Tr}\left[\left(\sum_{l=0}^{d^2-1} V_l^\dagger V_l\right)\rho\right] = \mathrm{Tr}[\rho]. \tag{A.16}$$

Evaluating the trace of a map on an element of some basis of $B(\mathcal{H})$ we get

$$\begin{aligned}\mathrm{Tr}[\mathcal{V}(|i\rangle\langle j|)] &= \mathrm{Tr}\left[\sum_{l=0}^{d^2-1} V_l|i\rangle\langle j|V_l^\dagger\right] = \mathrm{Tr}\left[\sum_{l=0}^{d^2-1} V_l^\dagger V_l|i\rangle\langle j|\right] \\ &= \sum_k \langle k| \left(\sum_{l=0}^{d^2-1} V_l^\dagger V_l|i\rangle\langle j|\right)|k\rangle = \left\langle j\left|\left(\sum_{l=0}^{d^2-1} V_l^\dagger V_l\right)\right|i\right\rangle.\end{aligned} \tag{A.17}$$

This result should be equal to $\delta_{i,j}$, since

$$\mathrm{Tr}[\mathcal{V}(|i\rangle\langle j|)] = \mathrm{Tr}[|i\rangle\langle j|] = \delta_{i,j}. \tag{A.18}$$

Therefore condition (A.15) is both sufficient and necessary for preserving the trace.

□

Choi-Kraus's theorem gives the most general form of CPT-maps. It is worth noting that operators V_i can be time dependent, as long as they condition (A.15) still holds. The next step is find equations for system evolution from these maps.

In order to find a master equation, it is necessary to find a generator $\mathcal{L}$ so that

$$\frac{d}{dt}\rho(t) = \mathcal{L}\rho(t). \tag{A.19}$$

Then the map can be written as $\mathcal{V}(t) = e^{\mathcal{L}t}$.

Firstly, we choose an orthonormal basis $\{F_i\}_{i=1}^{d^2}$ of $B(\mathcal{H})$

$$\langle\langle F_i|F_j\rangle\rangle \equiv \mathrm{Tr}\left[F_i^\dagger F_j\right] = \delta_{i,j}, \tag{A.20}$$

where $\langle\langle A|B\rangle\rangle = \mathrm{Tr}[A^\dagger B]$ is the standard operator scalar product in Fock-Liouville space. As the last basis element we choose a normalized identity element on $\mathcal{H}$: $F_{d^2} = \frac{1}{\sqrt{d}}\mathbb{1}_{\mathcal{H}}$. Because of this choice, all other basis elements have to be traceless. We can now expand operators V_i from Choi-Kraus's theorem into this basis

$$V_l(t) = \sum_{i=1}^{d^2} \langle\langle F_i|V_l(t)\rangle\rangle\, |F_i\rangle\rangle. \tag{A.21}$$

Applying into the form of $\mathcal{V}$ from eq. (A.14) on a general density matrix we get

$$\mathcal{V}(t)\rho = \sum_l \left[\sum_{i=1}^{d^2} \langle\langle F_i|V_l(t)\rangle\rangle\, F_i\rho \sum_{j=1}^{d^2} F_j^\dagger\, \langle\langle V_l(t)|F_j\rangle\rangle\right] = \sum_{i,j=1}^{d^2} c_{i,j}(t) F_i\rho F_j^\dagger, \tag{A.22}$$

where the coefficients $c_{i,j}(t) = \sum_l \langle\langle F_i|V_l\rangle\rangle\, \langle\langle V_l|F_j\rangle\rangle$ contain the summation over operators. Substituting this result into eq. (A.19) yields

$$\begin{aligned}
\frac{d\rho}{dt} &= \lim_{\Delta t\to 0}\frac{1}{\Delta t}(\mathcal{V}(\Delta t)\rho - \rho) = \lim_{\Delta t\to 0}\left(\sum_{i,j=1}^{d^2} c_{i,j}(\Delta t) F_i\rho F_j^\dagger - \rho\right) \\
&= \lim_{\Delta t\to 0}\left(\sum_{i,j=0}^{d^2-1} c_{i,j}(\Delta t) F_i\rho F_j^\dagger + \sum_{i=1}^{d^2-1} c_{i,d^2} F_i\rho F_{d^2}^\dagger\right. \\
&\left. + \sum_{j=1}^{d^2-1} c_{d^2,j}(\Delta t) F_{d^2}\rho F_j^\dagger + c_{d^2,d^2}(\Delta t) F_{d^2}\rho F_{d^2}^\dagger - \rho\right) \\
&= \lim_{\Delta t\to 0}\frac{1}{\Delta t}\left(\sum_{i,j=1}^{d^2-1} c_{i,j}(\Delta t) F_i\rho F_j^\dagger + \frac{1}{\sqrt{d}}\sum_{i=1}^{d^2-1} c_{i,d^2}(\Delta t) F_i\rho\right. \\
&\left. + \frac{1}{\sqrt{d}}\sum_{j=1}^{d^2-1} c_{d^2,j}(\Delta t)\rho F_j^\dagger + \frac{1}{d} c_{d^2,d^2}(\Delta t)\rho - \rho\right).
\end{aligned} \tag{A.23}$$

To eliminate time dependence, we define constants

$$\begin{aligned}
g_{i,j} &\equiv \lim_{\Delta t\to 0}\frac{c_{i,j}(\Delta t)}{\Delta t} \quad \left(i,j \neq d^2\right) \\
g_{d^2,d^2} &\equiv \lim_{\Delta t\to 0}\frac{c_{d^2,d^2}(\Delta t) - d}{\Delta t}.
\end{aligned} \tag{A.24}$$

Eq. (A.23) then takes on the form

$$\frac{d\rho}{dt} = \sum_{i,j=1}^{d^2-1} g_{i,j} F_i \rho F_j^\dagger + \frac{1}{\sqrt{d}} \sum_{i=1}^{d^2-1} g_{i,d^2} F_i \rho + \frac{1}{\sqrt{d}} \sum_{j=1}^{d^2-1} g_{d^2,j} \rho F_j^\dagger + \frac{g_{d^2,d^2}}{d} \rho. \tag{A.25}$$

By defining a new operator $F \equiv \frac{1}{\sqrt{d}} \sum_{i=1}^{d^2-1} g_{i,d^2} F_i$ we get

$$\frac{d\rho}{dt} = \sum_{i,j=1}^{d^2-1} g_{i,j} F_i \rho F_j^\dagger + F\rho + \rho F^\dagger + \frac{g_{d^2,d^2}}{d} \rho. \tag{A.26}$$

It is now useful to separate coherent Hermitian dynamics from incoherent parts. The operator F is split into hermitian (H) and anti-Hermitian (G) parts

$$F = \frac{F + F^\dagger}{2} + i\frac{F - F^\dagger}{2i} \equiv G - iH. \tag{A.27}$$

Substituting back into eq. (A.26) we obtain

$$\frac{d\rho}{dt} = g_{i,j} F_i \rho F_j^\dagger + \{G, \rho\} - i[H, \rho] + \frac{g_{d^2,d^2}}{d} \rho. \tag{A.28}$$

Defining the last auxiliary operator of this proof $G_2 \equiv G + \frac{g_{d^2,d^2}}{2d}$ simplifies

$$\frac{d\rho}{dt} = \sum_{i,j=1}^{d^2-1} g_{i,j} F_i \rho F_j^\dagger + \{G_2, \rho\} - i[H, \rho]. \tag{A.29}$$

To this point, we have only used the condition for complete positivity of the map. To include the property of preserving trace, we need to impose a condition

$$\mathrm{Tr}\left[\frac{d\rho}{dt}\right] = \mathrm{Tr}\left[\sum_{i,j=1}^{d^2-1} F_j^\dagger F_i \rho + 2G_2\rho\right] = 0. \tag{A.30}$$

Therefore G_2 has to fulfill

$$G_2 = \frac{1}{2} \sum_{i,j=1}^{d^2-1} g_{i,j} F_j^\dagger F_i \rho. \tag{A.31}$$

Substituting this condition back we get

$$\frac{d\rho}{dt} = -i[H, \rho] + \sum_{i,j=1}^{d^2} g_{i,j} \left(F_i \rho F_j^\dagger - \frac{1}{2} \left\{ F_j^\dagger F_i, \rho \right\} \right). \tag{A.32}$$

Since $g_{i,j}$ from a Hermitian matrix, it can be diagonalized. While also scaling the operator H we obtain the Lindblad form

$$\boxed{\frac{d}{dt}\rho(t) = \mathcal{L}(\rho) = -\frac{i}{\hbar}[H, \rho] + \sum_k \gamma_k \left[L_k \rho L_k^\dagger - \frac{1}{2} \left\{ L_k^\dagger L_k, \rho \right\} \right].} \tag{A.33}$$

B. Excitation by a δ-pulse

Consider a two-level system in an initial state $|\psi(t_0)\rangle$ at time t_0 with transition dipole moment μ between the two states under a laser pulse with $\vec{E}(t) = \vec{E}_0\delta(t-t_p)\frac{1}{2}\left(e^{-i\omega(t-t_p)}+e^{i\omega(t-t_p)}\right)$ located at time $t=t_p$ in the semiclassical approximation described in Chapter 1. The Hamiltonian for the system and laser interaction in the basis of the two levels is

$$H = H_S - \vec{\mu}\cdot\vec{E}(t)\begin{pmatrix}0&1\\1&0\end{pmatrix}. \tag{B.1}$$

The operator $\begin{pmatrix}0&1\\1&0\end{pmatrix}$ will be denoted k onward. In the interaction picture, the Hamiltonian takes on the form

$$H^{(I)} = -J_0\delta(t-t_p)\begin{pmatrix}1&0\\0&e^{i\omega(t-t_0)}\end{pmatrix}\begin{pmatrix}0&e^{i\omega(t-t_p)}\\e^{-i\omega(t-t_p)}&0\end{pmatrix}\begin{pmatrix}1&0\\0&e^{-i\omega(t-t_0)}\end{pmatrix} =$$

$$= \text{-J}_0\delta(t-t_p)\begin{pmatrix}0&e^{-i\omega(t_p-t_0)}\\e^{i\omega(t_p-t_0)}&0\end{pmatrix}, \tag{B.2}$$

where $J_0 = \frac{\vec{\mu}\cdot\vec{E}_0}{2}$. This Hamiltonian form can be conveniently written as

$$H^{(I)} = -J_0\delta(t-t_p)\tilde{k}, \tag{B.3}$$

where $U(t_0,t_p)\,kU(t_p,t_0) \equiv \tilde{k}$ and $U(t,t_0)$ is the backward time evolution operator from t_0 to t. It is important to note that $\tilde{k}$ is time-independent. The Schrödinger equation for the system in the interaction picture is

$$\frac{\partial}{\partial t}|\psi^I(t)\rangle = -\frac{i}{\hbar}H_I^{(I)}(t)|\psi^{(I)}(t)\rangle \tag{B.4}$$

The initial condition is the same for both the Schrödinger and the interaction picture, as $U(t_0,t_0)=1$. The formal solution takes on the form of a time-ordered exponential

$$|\psi^{(I)}(t)\rangle = \exp\left(-\frac{i}{\hbar}\int_{t_0}^{t}d\tau H_I^{(I)}(\tau)\right)|\psi(t_0)\rangle \tag{B.5}$$

When evaluating the integral, it is useful to look at expansions to different orders. In the second order, the integral can be solved by per partes method

$$\int_{t_0}^{t}d\tau H^{(t)}(\tau)\int_{t_0}^{\tau}d\tau' H^{(\tau)}(\tau') = \int_{t_0}^{t}d\tau\delta(\tau-t_p)\int_{t_0}^{t}d\tau'\delta(\tau'-t_p)J_0^2\tilde{k}^2 =$$

$$= J_0^2\hat{k}^2\int_{t_0}^{t}d\tau\delta(\tau-t_p)\Theta(\tau-t_p) = J_0^2\hat{k}^2\left[\Theta(\tau-t_p)\Theta(\tau+\gamma_p)\right]_{t_0}^{t} - \tag{B.6}$$

$$-J_0^2\hat{k}^2\int_{t_0}^{t}d\tau\Theta(\tau-t_p)\delta(\tau-t_p)$$

$$\Rightarrow\ I_2 = J_0^2\hat{k}^2\int_{t_0}^{t}d\tau\delta(\tau-t_p)\Theta(\tau-t_p) = \frac{1}{2}\Theta^2(t-t_p)J_0^2\tilde{k}^2 \tag{B.7}$$

For higher orders, a recurrent relation can be written

$$I_n = \int_{t_0}^{t} d\tau \delta\left(\tau - t_p\right) I_{n-1}\left(-J_0\right)\tilde{k} \tag{B.8}$$

From the per partes calculation and form of I_2 it can be seen that

$$I_n = \frac{1}{n!}\Theta^n\left(t - t_p\right)\left(-J_0\tilde{k}\right)^n \tag{B.9}$$

satisfies eq. (B.6). The evolution operator then has the form

$$U\left(t, t_0\right) = 1 + \sum_{n=1}^{\infty} \frac{1}{n!}\Theta^n\left(t - t_p\right)\left(-J_0\tilde{k}\right)^n \tag{B.10}$$

Returning back from the interaction picture, the

$$\begin{aligned} |\psi(t)\rangle &= U_0\left(t_1, t_0\right)\left|\psi^{(I)}(t)\right\rangle = U_0\left(t, t_0\right) U\left(t_1, t_0\right)|\psi\left(t_0\right)\rangle \\ &= U_0\left(t_1, t_0\right)\left(1 + \sum_{n=1}^{\infty} \frac{1}{n!}\hat{\Theta}\left(t - t_p\right) U_0\left(t_0, t_p\right)\hat{k}^n U_0\left(t_p, t_0\right)\left(-J_0\right)^n\right)|\psi\left(t_0\right)\rangle \end{aligned} \tag{B.11}$$

Since $|\psi(t_p)\rangle = U_0\left(t_p, t_0\right)|\psi(t)\rangle$ and $U_0\left(t, t_0\right) U_0\left(t_p, t_0\right) = U_0\left(t_p, t_0\right)$, the solution then becomes

$$\begin{aligned} &t > t_p : |\psi(t)\rangle = U_0\left(t, t_p\right) e^{-\frac{i}{\hbar}J_0 k} U_0\left(t_p, t_0\right)|\psi\left(t_0\right)\rangle \\ &t < t_p : |\psi(t)\rangle = U_0\left(t, t_0\right)|\psi\left(t_0\right)\rangle \end{aligned}$$

The exponential can be easily calculated by diagonalizing, as the matrix has a simple and known spectrum. The obtained operator for excitation then becomes

$$\hat{Ex} = e^{-\frac{i}{\hbar}J_0 k} = \frac{1}{2}\begin{pmatrix} 1 & 1 \\ -1 & 1 \end{pmatrix}\begin{pmatrix} \exp i\frac{J_0}{\hbar} & 0 \\ 0 & \exp -i\frac{J_0}{\hbar} \end{pmatrix}\begin{pmatrix} 1 & -1 \\ 1 & 1 \end{pmatrix} \tag{B.12}$$

$$\boxed{\hat{Ex} = \begin{pmatrix} \cos\frac{J_0}{\hbar} & -i\sin\frac{J_0}{\hbar} \\ -i\sin\frac{J_0}{\hbar} & \cos\frac{J_0}{\hbar} \end{pmatrix}.} \tag{B.13}$$